

Amphibolitic rocks from the Precambrian of Grand Canyon: mineral chemistry and phase petrology

MALCOLM D. CLARK

Department of Geology, University of Leicester, England

SUMMARY. The amphibolites and mafic schists that occur in the Precambrian metamorphic rocks of the Grand Canyon are divided into five major groups: anthophyllite and cordierite-anthophyllite rocks, early amphibolites, Granite Park mafic complex, hornblende-bearing dykes, and tremolite-bearing dykes. Many types of amphibole occur in these rocks. Microprobe analyses identify gedrite, anthophyllite, cummingtonite, and grunerite, as well as three groups of calcic amphiboles. These last range in composition from colourless tremolitic or actinolitic amphiboles, through pale-green hornblende, to strongly pleochroic green-brown hornblende, which contains a significant proportion of the tschermakite and pargasite endmembers. Phase relationships between the coexisting amphiboles and other minerals are presented for two regional metamorphic events. Assemblages containing chlorite, garnet, and hornblende were formed during the first event; from the absence of staurolite, but the presence of almandine garnet and oligoclase-andesine, it is concluded that the metamorphic grade was between the upper greenschist and the lower amphibolite facies. The second period of metamorphism produced rocks of the staurolite and sillimanite zones, within which three main 'subfacies' can be distinguished on the basis of phase relationships in the mafic schists.

'OLDER Precambrian' metamorphic and igneous rocks, 1400 to 2000 Ma in age, are exposed within the Upper and Lower Granite Gorges of the Grand Canyon, and at isolated localities between. The total length of outcrop along the Colorado River is over 144 km, and there is further considerable exposure within side-canyons. In recent years these rocks have been intensively studied by the author and his associates, R. S. Babcock and E. H. Brown from Western Washington State University, Bellingham, and D. E. Livingston from the University of Arizona. The crystalline rocks of the region have been divided into widespread schists and associated lithologies (the Vishnu Group), a suite of intrusive granitic rocks (the Zoroaster Plutonic Complex), a layered mafic complex (the Granite Park Mafic Body), and two distinctive units of gneiss (the

Trinity and Elves Chasm Gneisses). Metamorphic grade in the Grand Canyon ranges from lowermost to upper amphibolite facies. Details of the geology are given on two maps of the Older Precambrian by Clark *et al.* (1976, 1977) and in Babcock *et al.* (1974, 1977), and Clark (1977). The location of the Upper and Lower Granite Gorges and localities mentioned in the text are shown in fig. 1.

The amphibolites and mafic schists that occur in the Older Precambrian rocks are subdivided into five major groups on the basis of field occurrence and mineral composition: anthophyllite (gedrite)-bearing rocks; early amphibolites (plagioclase-hornblende-bearing); Granite Park mafic complex; hornblende-bearing dykes; and tremolite-bearing dykes. Representative mineral assemblages are listed in Table I (Miniprint, pp. M23-5). The nature and origin of these mafic rocks were outlined in a previous paper (Clark, 1977). This report presents complementary details of the mineral chemistry and phase relationships.

Petrology

Anthophyllite-bearing rocks. Rocks of unusual bulk composition, which are mainly anthophyllite-bearing, are divided into three subgroups on the basis of field appearance and mineralogy: cordierite-anthophyllite rocks, which contain quartz, cordierite, and anthophyllite but lack plagioclase; biotite is ubiquitous and garnet is common; such rocks form competent units up to several metres wide, some of which are conspicuously layered. Anthophyllite schists and paragneisses, which contain plagioclase as an essential constituent; biotite, cordierite, and garnet are common, and cumming-

¹ Since anthophyllite and gedrite cannot readily be distinguished by optical means, the general name anthophyllite is used for both minerals in all routine field and petrographic descriptions herein.

tonite occurs in some rocks; the anthophyllite schists and paragneisses show a pronounced compositional layering in the field, and gradations between lithologies can be observed over a few centimetres. And rocks that contain cummingtonite rather than anthophyllite, and are typified by the assemblage cummingtonite-garnet-biotite-quartz \pm plagioclase; their most distinctive feature is the abundance of garnet, which constitutes 50 to 80% by volume.

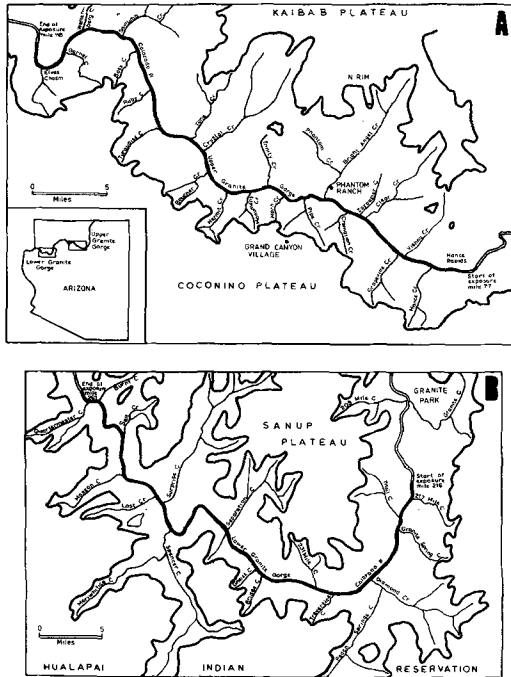


FIG. 1. Extent of Upper and Lower Granite Gorges and location of major side-canyons.

Anthophyllite is the most common amphibole and occurs as dark needles and radial and columnar aggregates up to several centimetres long, which are oriented parallel to the schistosity in the schistose rocks but which are more randomly oriented in massive lithologies. Cummingtonite displays multilamellar twinning, which, together with angular extinction, helps to distinguish it from anthophyllite. In specimen BA2N cummingtonite and anthophyllite are present, but cummingtonite is generally uncommon. Biotite is always subordinate to anthophyllite in the cordierite-anthophyllite rocks.

Cordierite is mostly untwinned, is partly pinitized, and interlocks with quartz in cordierite-anthophyllite rocks and with quartz and plagioclase in anthophyllite schists and paragneisses. Rounded cordierite porphyroblasts up to 1 cm

across are common. An unusual occurrence of cordierite is at Travertine Canyon, Lower Granite Gorge, where it occurs as large prismatic crystals several centimetres long; radial aggregates of anthophyllite and blades of biotite are intergrown, and the prisms are sieved with quartz inclusions. Similar occurrences, in which cordierites are elongate parallel to the *c*-axis, have been recorded near Texas Creek, Colorado, by Travis (1956) and near Dixon, New Mexico, by Montgomery (1953). Garnet forms large porphyroblasts up to several centimetres across, which are often concentrated in distinct layers. Some porphyroblasts are skeletal and indented, deflect the foliation, and are apparently pre- to syntectonic in age; others have sharply defined cross-cutting margins indicating post-tectonic growth. Commonly, the garnetiferous layers are biminerale and comprise a mosaic of skeletal garnet including quartz. Textures show garnet to be compatible with anthophyllite and cordierite where the three phases are associated together. Magnetite, ilmenite, or both occur in all of the observed assemblages. Plagioclase is often sericitized, and late chlorite is sometimes present.

Cordierite-anthophyllite rocks and associated mafic schists represent 'quasi' sedimentary types, which attained their bulk composition prior to metamorphism. They were derived in varying degrees from basic igneous materials that had suffered intense alteration and loss of lime and alkalis, probably by reaction with sea water. For a discussion of the origin of these rocks see Clark (1977).

Early amphibolites that form part of the Vishnu succession are subdivided into two groups: well-defined competent layers more than 1 m and up to many tens of metres thick, mainly composed of plagioclase and hornblende \pm subordinate quartz, biotite, clinopyroxene, and epidote. And schistose units, a few centimetres to 1 or 2 m thick, in which plagioclase and hornblende predominate; quartz and biotite are always present, but variable in abundance, and garnet is common; cummingtonite occurs in some rocks.

Microscopically, hornblende (35 to 65%) is typically green or green-brown, but tremolitic or actinolitic varieties are paler (see later). Cummingtonite, in association with hornblende, is untwinned, and this is a contrast to the well-twinned cummingtonite in the anthophyllite assemblages; it is pale green or pale brown, and therefore shows a marked colour contrast in thin section to the coexisting hornblende. Clinopyroxene is rare, tending to form predominantly monomineralic areas enclosed in normal amphibolite.

Field and chemical considerations indicate that the early amphibolites represent a series of basic

lava flows and tuffs deposited in an area of active sedimentation.

The *Granite Park mafic complex* at mile¹ 209 is a fault-bounded exposure of the Older Precambrian. The mafic complex that occurs here and in a shorter section at mile 212 comprises a variety of lithologies: these include medium-grained meta-leucogabbro, which predominates, meta-trondhjemite, meta-anorthosite, amphibolite, and meta-gabbroic pegmatite. These rocks form a layered sequence with compositional variations on the scale of centimetres to metres.

Calcic amphibole is the dominant mafic mineral, ranging from colourless tremolite to green hornblende, although the composition shows a direct relation to the lithology: in gabbroic and anorthositic rocks (i.e. in rocks containing a high proportion of plagioclase) tremolite is the common amphibole, forming colourless or pale green fibrous laths and rarely lamellar twinned crystals. In contrast, darker green hornblende is restricted to the amphibolites. Other, minor phases are biotite, epidote, and magnetite.

Field and chemical data for the Granite Park mafic complex strongly suggest that it originated as a layered series of plagioclase-rich cumulates (Clark, 1977).

The *hornblende-bearing dykes* are either of normal amphibolite with plagioclase and hornblende, usually with subordinate quartz, biotite, epidote, and magnetite, or they are composed of hornblende only plus minor opaques. These ultrabasic dykes are rare.

Hornblende-bearing dykes or sills are scattered throughout the Lower Precambrian rocks. They form concordant or rarely cross-cutting layers in the Vishnu Group, and are conspicuous in several of the older granitic plutons such as the Zoroaster, Ruby, and Diamond Creek plutons, and in the Trinity and Elves Chasm Gneisses. Dyke intrusion occurred after the emplacement of these bodies, but prior to the period of medium to high-grade regional metamorphism, dated at 1650 ± 25 Ma ago (Livingston *et al.*, 1974).

The *tremolite-bearing dykes* contain tremolite, talc, chlorite, biotite, and minor plagioclase, and occur sparsely within the Vishnu Group, with occurrences at miles 78.2 and 83, and at the mouth of Clear Creek (mile 84). Microscopically, pale-green, lamellar-twinned crystals of tremolite are common and are associated with talc. No relationships have been found between tremolite-bearing and hornblende-bearing dykes to indicate a relative age of intrusion.

¹ Mileage represents the distance along the Colorado River from Lees Ferry at the start of the Grand Canyon.

Mineral chemistry

Mineral analyses were performed on a Cambridge Instruments Microscan V electron micro-probe at the University of Leicester. Elements were analysed in pairs (starting with Na and K) at 15 kV and *c.* 0.02 μ A specimen current, using synthetic and natural standards. Corrections to the raw data were made with a modified version of the program M.A.G.I.C.IV (after Colby, 1968, 1971). The percentage end-members of garnets were determined with a program from the University of Durham (written by Peckett after Rickwood, 1968). The compositions of plagioclase, amphibole, garnet, cordierite, biotite, and talc are given in Tables II to VI (pp. M23-5). Other tables of recalculated data are available on request. Most analyses represent an average of five points or more per grain, and are accurate to within about 2%. The lower limits of detection range from about 0.02 to 0.05%. Total iron from microprobe analyses is reported as FeO, the significance of which is discussed below for individual minerals.

Plagioclase. Both the early amphibolites (S11A; W4A; 17A-71; 17B-71) and the hornblende-bearing dykes (G1R) have plagioclase in the andesine range, but with individual zones as high as An₅₉. Lower An contents, around An₂₄, occur in anthophyllite schists (BA2N), and apparently reflect the low Ca content of the bulk rocks. Somewhat surprising is the plagioclase from the tremolite-bearing dyke at mile 83 (57-2F), which averages An₃. This is incompatible with the basic-ultrabasic character of the dyke, and can only be accounted for by late, low-temperature alteration.

In contrast to the above amphibolites, some layers in the Granite Park mafic complex contain plagioclases that have apparently retained their original igneous composition: bytownite occurs in layers of meta-gabbro and meta-anorthosite (73/GP3), labradorite in amphibolites (GP2), and andesine in trondhjemites (GP4). The total range in composition is about An₃₀ to An₈₅.

Zoning in plagioclase is not marked, is usually normal, and the maximum range in any one specimen is about An₂₀.

Amphibole. Five analysed ortho-amphiboles are anthophyllites and five are gedrites. These two minerals cannot be distinguished by optical means, but are defined chemically as the Al-poor and Al-rich ortho-amphiboles (Rabbitt, 1948; Deer *et al.*, 1963; Robinson and Jaffe, 1969; Stout, 1972), and those analysed have limits at 0.9 and 2.0 Al atoms per formula unit. The relative concentrations of Mg and Na also help to separate anthophyllite from gedrite in the present study.

Unlike the ortho-amphiboles, cummingtonite

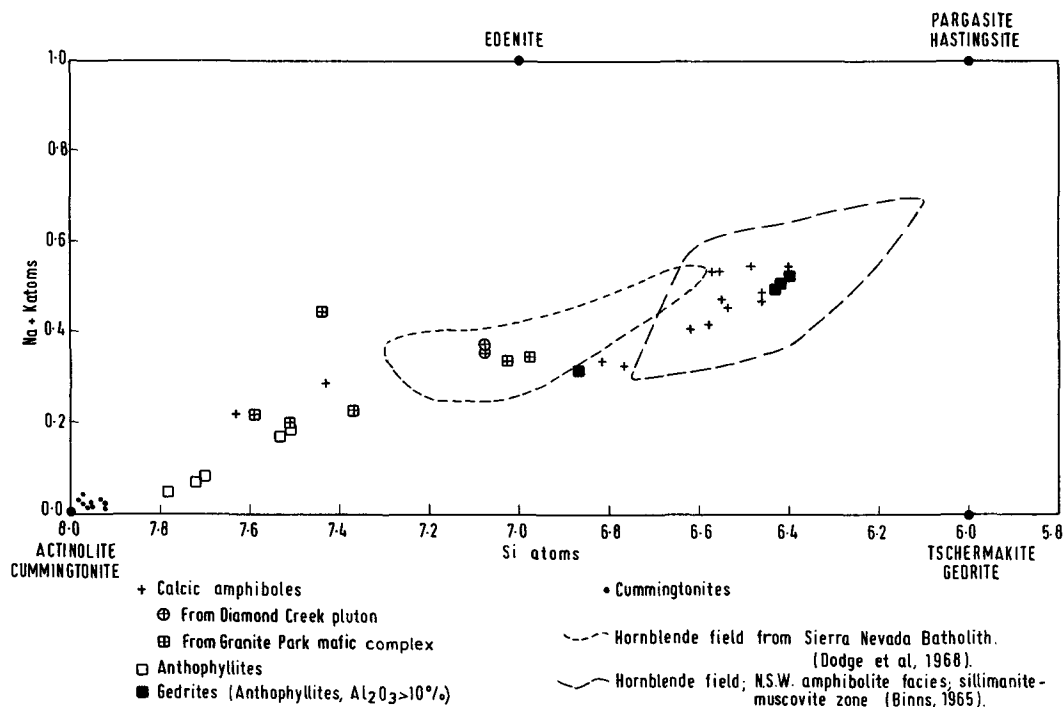


FIG. 2. Classification of amphiboles. Na + K versus Si atoms per formula unit for analysed amphiboles (from Robinson and Jaffe, 1969; after Hallimond, 1943, and Leake, 1968). Cummingtonite plots include grunerite.

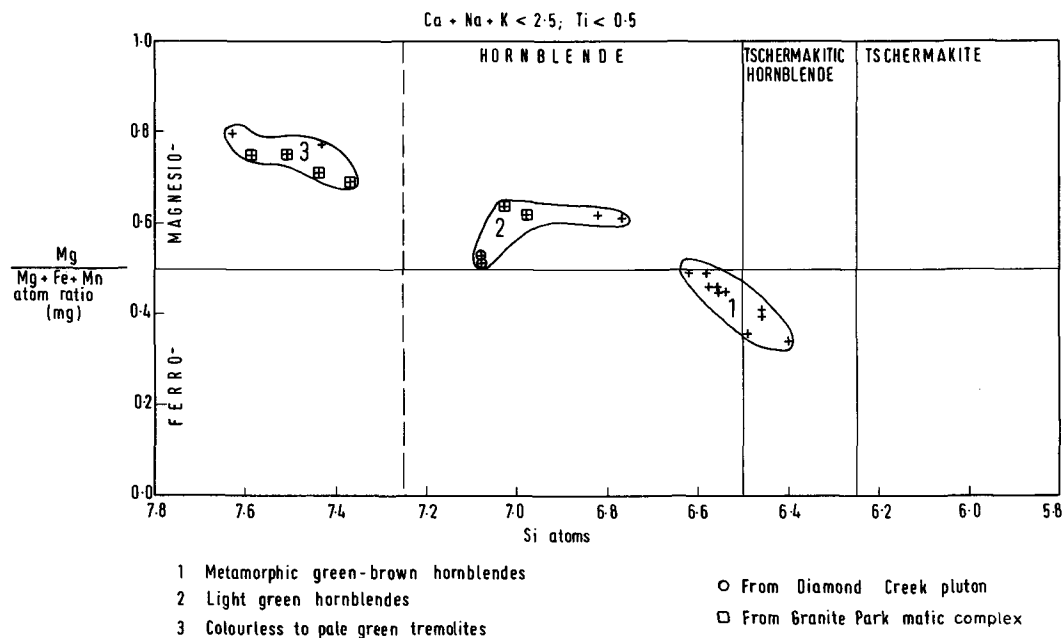


FIG. 3. Classification of calcic amphiboles. Mg/(Mg + Fe + Mn) versus Si atoms per formula unit (after Leake, 1968). Less than 2.5 atoms of (Ca + Na + K); less than 0.5 atoms of Ti per 23 oxygen atoms in the water-free formula.

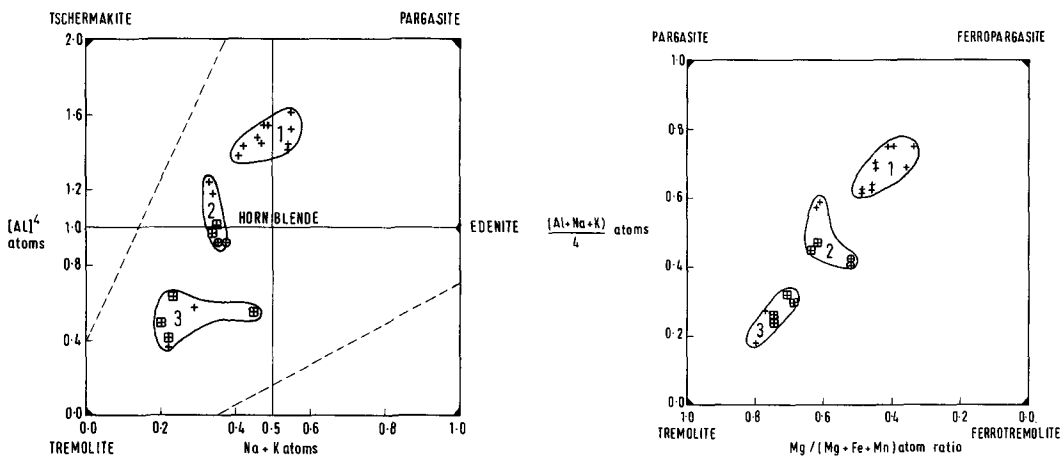
and grunerite form a continuous series based on the substitution of Fe and Mg. Jaffe *et al.* (1961) divided the series midway with Mg > Fe as cummingtonite and Mg < Fe as grunerite. Four analyses have about equal Fe and Mg, and two of these can be classified as grunerites; all four are untwinned and coexist with hornblende \pm garnet at Travertine Canyon (samples 17A-71 and 17B-71). In contrast, the other five analyses contain more Mg than Fe, and are therefore cummingtonites. They are well twinned and are associated with anthophyllite in sample BA2N and with garnet in P3B. It would therefore appear that the compositional variations are a direct reflection of the composition of the coexisting minerals, and this observation is borne out by the phase relationships shown in fig. 7.

Fig. 2 shows the progressive increase in Na + K with fall of Si content in the amphiboles. Three methods of classifying the calcic amphiboles are used because of the complexity of element substitution; each uses different parameters, such that different features of the amphiboles are illustrated. In all plots the amphiboles fall into three groups, the significance of which is discussed in the concluding remarks. In fig. 3 the division into three groups occurs both on the Si content and on the mg ratio. The lack of iron enrichment in the Granite Park mafic body (Clark, 1977) is reflected in the iron content of the associated amphiboles; all lie in the Mg-rich half of the figure and include four of the six analyses from group 3. Fig. 4 shows a wide range in Al^{iv} substitution with three distinct groups,

of which one could be called tremolite. Fig. 5 confirms the threefold grouping.

The grouping of the calcic amphiboles into three compositional types in figs. 3-5 can be related to their microscopic appearance. Group 1 amphiboles are hornblendes containing a significant proportion of tschermakite and pargasite end-members. They have a high degree of substitution of Al for Si, contain between 0.4 and 0.6 (Na + K) atoms, and are iron-rich. As a consequence, these amphiboles show a marked green-brown pleochroism in thin section, and fall in the metamorphic field outlined by Binns (1965) in fig. 2. Group 2 amphiboles fall closest in all plots to average hornblende, and as a result of a lower Fe/Mg ratio are less strongly coloured; these are light-green hornblendes, and include the two analyses from the Diamond Creek pluton and two from the Granite Park mafic complex. Calcic amphiboles of the third group fall at the opposite end of the spectrum to those of group 1. They show a low degree of Si:Al substitution, are Mg-rich, and are tremolites containing a proportion of the 'hornblende' molecule. Microscopically they are colourless to pale green, commonly exhibit lamellar twinning, and can be provisionally identified as tremolites from their appearance. Included in this group are four of the six analyses from Granite Park and both analyses from the tremolite-bearing dyke at mile 83.

In conclusion, the colour and composition of the calcic amphiboles are primarily a function of bulk rock composition. All but two analyses are from



FIGS. 4 and 5. Classification of the calcic hornblendes. 1. Metamorphic green-brown hornblendes. 2. Light-green hornblendes. 3. Colourless to pale-green tremolites. \oplus from Diamond Creek pluton. \boxplus from Granite Park mafic complex. FIG. 4 (left). After Deer *et al.*, 1963. Al^{iv} vs. Na + K atoms per formula unit. The dashed lines show the limits of composition plotted by Deer *et al.* FIG. 5 (right). After Ernst (1968) as modified by Windley and Smith (1974). (Al + Na + K)/4 vs. Mg/(Mg + Fe + Mn). Since electron microprobe analysis does not yield the amount of Fe³⁺, (Al + Na + K) is used rather than (Al + Na + Fe³⁺) atoms per 4 formula units.

amphibolites and mafic schists of approximately the same metamorphic grade (middle to upper amphibolite facies), so that the effects of increasing temperature on colour and Fe/Mg distribution cannot be ascertained.

Garnet. Although total iron from electron microprobe analysis is calculated as Fe^{2+} , the amount of Fe^{3+} in garnet can be estimated fairly well from the deficiency of trivalent elements after Al has been considered. There is virtually no Fe^{3+} substituting for Al, and so the andradite component is regarded as negligible for all garnets (see also discussion by Brown, 1967, and by Muller and Schneider, 1971). The garnets analysed are plotted

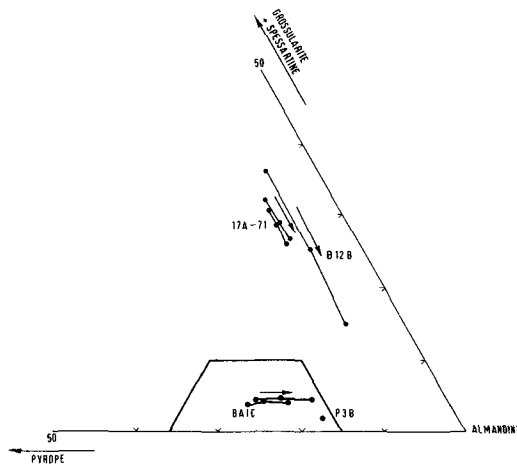


FIG. 6. Composition of analysed garnets as mol. % of the end-members almandine, pyrope, grossular + spessartine. Arrows indicate zoning from core to rim. Line encloses field of garnet + cordierite from Wynne-Edwards and Hay (1963).

on fig. 6. There are two from a cordierite-anthophyllite rock (BA1C), one from a garnet-cummingtonite rock (P3B), and two from a cummingtonite-hornblende mafic schist (17A-71). In addition, one analysis from a K-poor schist (B12B) is included for comparison. A wide range of bulk compositions is therefore considered, with the garnets plotting in two groups corresponding to differences in metamorphic grade (Muller and Schneider, 1971). Garnets from samples BA1C and P3B were formed at a higher grade and contain less spessartine and more almandine than those from 17A-71 and B12B. This separation, at least in part, can also be related to factors of mineralogy and rock composition. On the other hand, all the garnets are zoned, and show an increase in the almandine component from core to rim. Brown (1969) adequately demonstrated that

such a pattern may reflect Mn-depletion during garnet growth at constant grade, and/or increase in metamorphic grade, with higher Fe occurring in progressively formed zones. The latter may also be associated with a corresponding decrease in Ca and so is largely consistent with the present data. It should be noted that only specimen B12B shows appreciable Mn-depletion from core to rim, but this is also associated with a decrease in Ca.

The Fe-Mg phases that coexist with garnet are a reflection of the bulk composition. Wynne-Edwards and Hay (1963) outlined the field where garnet and cordierite coexist, and this is shown on fig. 6. Garnets from BA1C (which coexist with cordierite) fall within this field, but those from 17A-71 and B12B (with no cordierite) lie outside. Eskola (1915) first suggested that there is a limit to the amount of iron that can be accommodated in cordierite, and that almandine appears with cordierite when this limit is exceeded. Wynne-Edwards and Hay (1963) indicated a limit of between 27.1 and 29.5% iron molecule for cordierite of the Westport area, Ontario, but this value depends on the metamorphic environment. Thus, garnet coexisting with cordierite appears to have a restricted field of composition close to the almandine end-member. The Ca content of garnet also shows a direct relationship to the composition of the coexisting phases, and this is illustrated in a general way by the phase relationships in fig. 7. Garnets coexisting with cummingtonite and hornblende (17A-71) are more calcic than those that coexist with gedrite and cordierite (BA1C). The above two examples suffice to show that the distribution of analyses on fig. 6 is dependent to at least some extent on mineralogy, and therefore on rock composition.

In conclusion, it would appear that differences in both temperature of formation and bulk rock composition are responsible for the observed variations in the composition of the analysed garnets. In addition, the pattern of zoning may be explained by an increase in metamorphic grade during the period of garnet growth.

Other minerals. Analyses of cordierite, biotite, and talc are given in Table VI (page M25).

Phase relationships

The phase relationships in a variety of mafic rocks from the Vishnu Group are presented in figs. 7 and 8. These diagrams are based on petrographic observations although the composition of some of the key assemblages was confirmed by microprobe analysis. The method of projection and compositional fields are from Robinson and Jaffe (1969), but both anthophyllite and gedrite are represented by the general field of orthoamphibole.

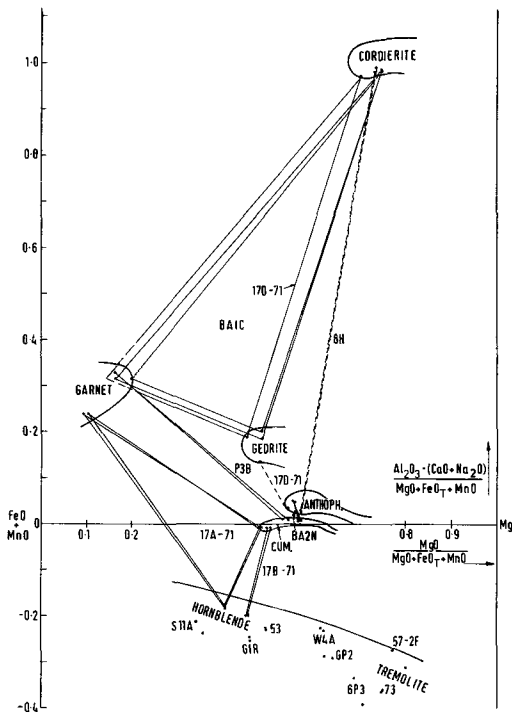


FIG. 7. Phase relationships of coexisting amphiboles, garnet, and cordierite in mafic rocks from the staurolite-sillimanite and sillimanite-muscovite zones. Method of projection after Stout (1972). Stability fields of phases modified after Stout (1972). Dashed tie-lines indicate uncertainty of phase relationships. Middle and upper amphibolite facies only.

The graphical representation of amphibole compositions and assemblages has long been a major problem. In both figs. 7 and 8, a planar representation of assemblages is obtained by projecting through plagioclase, which is regarded as a ubiquitous phase for practical purposes. A similar 'feldspar' projection was used by Green (1960), and the procedure was described algebraically by Korzhinskii (1959). In fig. 7 the system $\text{Al}_2\text{O}_3\text{-FeO-Fe}_2\text{O}_3\text{-MnO-MgO-SiO}_2\text{-CaO-Na}_2\text{O-H}_2\text{O}$ is considered; it is assumed that SiO_2 and Fe_3O_4 are present in excess as the phases quartz and magnetite, and that H_2O is perfectly mobile. The remaining components can be shown in the form of a compositional tetrahedron (Stout, 1972, fig. 16), and the plane of projection chosen contains the $(\text{FeO} + \text{MnO})\text{-MgO}$ edge of the tetrahedron and is parallel to the $\text{Al}_2\text{O}_3\text{-(CaO} + \text{Na}_2\text{O)}$ edge. In practice, the molecular ratio $(\text{Al}_2\text{O}_3 - (\text{CaO} + \text{Na}_2\text{O})) / (\text{MgO} + \text{FeO} - \text{Fe}_2\text{O}_3 + \text{MnO})$ is plotted against $\text{MgO} / (\text{MgO} + \text{FeO} - \text{Fe}_2\text{O}_3 +$

$\text{MnO})$, although it should be noted that FeO_t was used in the present study rather than $\text{FeO-Fe}_2\text{O}_3$. Using FeO_t shifts the position of the calcic amphiboles to slightly more Fe-rich compositions. Other phases are regarded as containing negligible Fe_2O_3 and will be unaffected. Calcic amphiboles and some of the cummingtonites have $\text{CaO} + \text{Na}_2\text{O}$ in excess of Al_2O_3 , and thus plot in the negative portion of the projection. Other amphiboles, plus garnet and cordierite, plot in the positive portion (phases that contain no Fe or Mg project at infinity). The advantage over the triangular projection of Robinson and Jaffe (fig. 8) is that 'coexisting pairs for which there is no fractionation of Mg and Fe are indicated by vertical tielines, whereas positive or negative slopes of tielines indicate that one member of a pair has a greater or lesser $\text{MgO} / (\text{MgO} + \text{FeO})$ ratio than the other member' (Stout, 1972, p. 135). Either projection is useful, however, in that the compositional fields of gedrite, anthophyllite, cummingtonite, and the calcic amphiboles can be portrayed on one plane.

Robinson and Jaffe (1969) pointed out that the projections of assemblages are only true phase diagrams if the following three conditions are met: the assemblage contains quartz and plagioclase (and magnetite in this case); the plagioclase composition has no influence on the amphibole composition; and components other than those used in the projection are negligible. All three requirements are rarely fulfilled, but the resulting diagrams are of great use in comparing assemblages.

A brief mention should be made of two assemblages in fig. 7 that are somewhat anomalous. 17D-71 contains the assemblage cordierite-garnet-gedrite, but analyses indicate that lamellae of anthophyllite are also present in association with gedrite; the latter has lower Al_2O_3 than the gedrite that coexists with cordierite and garnet. Similar irregularities in the composition of orthoamphibole have been noted by other workers, and may be explained as either primary features of growth (cf. Stout, 1972; Chinner and Fox, 1974) or as exsolution features (cf. Ross *et al.*, 1969; Robinson *et al.*, 1971). However, present data do not allow a distinction between the two alternatives. Secondly, 8H shows an association of cordierite with anthophyllite, but possibly not enough analyses were made to see if gedrite is also present. Both 8H and 17D-71 are from Travertine Canyon.

Relationship with metamorphic events. The crystalline rocks of the Grand Canyon have suffered two periods of progressive regional metamorphism, the evidence for which was outlined by Brown *et al.* (1977). Near Boucher Creek two

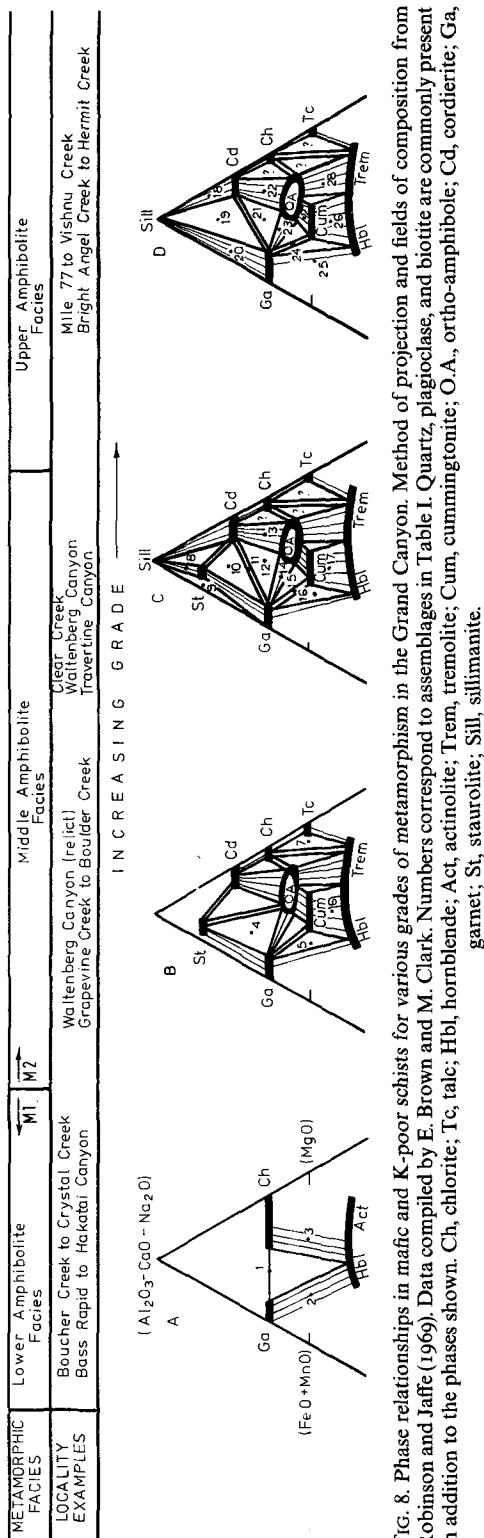


FIG. 8. Phase relationships in mafic and K-poor schists for various grades of metamorphism in the Grand Canyon. Method of projection and fields of composition from Robinson and Jaffe (1969). Data compiled by E. Brown and M. Clark. Numbers correspond to assemblages in Table I. Quartz, plagioclase, and biotite are commonly present in addition to the phases shown. Ch, chlorite; Act, actinolite; Trem, tremolite; Cum, cummingtonite; O.A., ortho-amphibole; Cd, cordierite; Ga, garnet; St, staurolite; Sill, sillimanite.

underformed granitic plutons, provisionally dated at 1912 ± 70 Ma and 2013 ± 116 Ma (Rb-Sr ages; data in Babcock *et al.*, 1977) intrude relatively low grade metamorphic rocks, implying that there was a period of metamorphism prior to their intrusion.

Rocks from this first metamorphic event are now preserved as 'windows' between Boucher and Crystal Creeks and between Bass Rapid and Hakatai Canyon. Elsewhere in the Grand Canyon the prevailing grade of metamorphism is within the staurolite and sillimanite zones of the amphibolite facies, and all plutons older than 1650 Ma are strongly foliated. A second period of metamorphism can therefore be implied, dated by Livingston *et al.* (1974) at 1650 ± 25 Ma by Rb-Sr isochron techniques.

Both periods of metamorphism are represented in fig. 8. Diagram A shows that assemblages containing garnet, chlorite, and hornblende were formed in mafic and K-poor schists during the first event. On the basis of the absence of staurolite but the presence of almandine garnet and plagioclase $> An_{15}$, Table II, it is concluded that the grade of metamorphism was close to the boundary between the upper greenschist and lower amphibolite facies. Winkler (1976) stated that both the first appearance of plagioclase and that of staurolite and/or cordierite at a slightly higher temperature have been used by different workers to mark the beginning of the amphibolite facies. Although the choice is arbitrary, the rocks between Boucher and Crystal Creeks and between Bass Rapid and Hakatai Canyon are here included in the lowermost amphibolite facies on the basis of the presence of plagioclase. This is also in accordance with previously published work by the author and his colleagues (cf. Clark *et al.*, 1976; Brown *et al.*, 1977).

Other diagrams on fig. 8 show the phase relationships deduced for the second period of regional metamorphism. Three main 'sub-facies' can be distinguished, based on the formation and breakdown of staurolite, and on the presence or absence of sillimanite. Phase relationships shown in diagram C are similar to those recorded by Stout (1972) in mafic schists at Telemark, Norway. It is also likely that cummingtonite and ortho-amphibole were not formed at exactly the same temperature.

Acknowledgements. The writer thanks Drs. R. S. Babcock and E. H. Brown of Western Washington State University and Drs. T. D. Ford and B. F. Windley of the University of Leicester for their help during the course of the research and for reviewing the manuscript. Appreciation is also extended to Mr. R. N. Wilson for his help with microprobe analysis. Grants towards the research were given by N.E.R.C. and the Museum of Northern Arizona.

REFERENCES

- Babcock (R. S.), Brown (E. H.), and Clark (M. D.), 1974. In Breed (W. J.) and Roat (E. C.) (eds.), *Geology of the Grand Canyon*, ch. 7, pp. 2-19. Mus. N. Ariz., Flagstaff, and Grand Canyon Nat. Hist. Assoc.
- Clark (M. D.), Brown (E. H.), and Livingston (D. E.), 1977. Unpublished MS.
- Binns (R. A.), 1965. *Mineral. Mag.* **35**, 308-26.
- Brown (E. H.), 1967. *Contrib. Mineral. Petrol.* **13**, 259-92.
- 1969. *Am. Mineral.* **54**, 1662-877.
- Clark (M. D.), and Babcock (R. S.), 1977. Unpublished MS.
- Chinner (G. A.) and Fox (J. S.), 1974. *Geol. Mag.* **111**, 397-508.
- Clark (M. D.), 1977. Unpublished MS.
- Babcock (R. S.), and Brown (E. H.), 1976. *Geologic map of the Grand Canyon National Park, Arizona (Older Precambrian geology)*. Grand Canyon Nat. Hist. Assoc. and Mus. N. Ariz., Flagstaff.
- Brown (E. H.), and Babcock (R. S.), 1977. *Geologic map of the western Grand Canyon, Arizona (Older Precambrian geology)*. In press.
- Colby (J. W.), 1968. *Advances in X-ray Analysis*, **11**, 287-305.
- 1971. Magic IV—a computer program for quantitative electron microprobe analysis. Unpublished MS., Bell Telephone Labs.
- Deer (W. A.), Howie (R. A.), and Zussman (J.), 1963. *Rock-forming Minerals*. Longmans, London.
- Dodge (F. C. W.), Papike (J. J.), and Mays (R. E.), 1968. *J. Petrol.* **9**, 378-410.
- Ernst (W. G.), 1968. *Amphiboles*. Springer Verlag, New York.
- Eskola (P.), 1915. *Bull. Comm. Geol. Finlande*, no. 44, 109-413.
- Green (J. C.), 1960. *Geology of the Errol Quadrangle, New Hampshire—Maine*. Ph.D. thesis, Harvard University.
- Hallimond (A. F.), 1943. *Am. Mineral.* **28**, 65-89.
- Jaffe (H. W.), Groenevald Meyer (W. O. J.), and Selchow (D. H.), 1961. *Ibid.* **46**, 642-53.
- Korzhinskii (D. S.), 1959. *Physicochemical basis of the analysis of the paragenesis of minerals*. New York Consultants Bur.
- Leake (B. E.), 1968. *Geol. Soc. Am. Spec. Pap.* 98.
- Livingston (D. E.), Brown (E. H.), Babcock (R. S.), and Clark (M. D.), 1974. *Geol. Soc. Am., Abstr. with programs*, **6**, 848-9.
- Montgomery (A.), 1953. *New Mexico Bur. Mines Mineral Res. Bull.* **30**.
- Muller (G.) and Schneider (A.), 1971. *Contrib. Mineral. Petrol.* **31**, 178-200.
- Rabbitt (J. C.), 1948. *Am. Mineral.* **33**, 263-323.
- Rickwood (P. C.), 1968. *Contrib. Mineral. Petrol.* **18**, 175-98.
- Robinson (P.) and Jaffe (H. W.), 1969. *Mineral. Soc. Am. Spec. Pap.* **2**, 251-74.
- Klein (C.), and Ross (M.), 1969. *Contrib. Mineral. Petrol.* **22**, 248-58.
- Ross (M.), and Jaffe (H. W.), 1971. *Am. Mineral.* **56**, 1005-41.
- Ross (M.), Papike (J. J.), and Shaw (K. W.), 1969. *Mineral. Soc. Am. Spec. Pap.* **2**, 275-99.
- Stout (J. H.), 1972. *J. Petrol.* **13**, 99-145.
- Travis (R. B.), 1956. *Am. Mineral.* **41**, 796-9.
- Windley (B. F.) and Smith (J. V.), 1974. *Bull. Grønlands Geol. Unders.*, no. 108.
- Winkler (H. J. F.), 1976. *Petrogenesis of metamorphic rocks*. Springer Verlag, New York.
- Wynne-Edwards (H. R.) and Hay (P. W.), 1963. *Can. Mineral.* **7**, 453-78.

[Manuscript received 2 December 1977]

M. D. Clark: Rocks from Grand Canyon (App.) M23

Table I. Representative mineral assemblages in mafic and K-poor rocks

Quartz	x	x	x	x	x	x	x	x	x	x	x	x	x	x	x	x	x	x	x	x
Plagioclase	x	x	x	x	x	x	m	m	x	x	x	x	x	x	x	x	x	x	x	x
Chlorite	x		x				x													x
Talc							x													x
Biotite	x	x	x	x	x	x	x	x	x	x	x	x	x	x	x	x	x	x	x	m
Garnet	x	x	x	x			x	x	m	x	x	x	x	x	x	x	x			x
Cordierite							x	m	x	x			x	x		x	x			
Staurolite			x				x	m	x											
Sillimanite							x	x						x	x	x				
Trem./Act.		x				x														
Hornblende	x			x	x															x
Cummingtonite				x	x					x								x	x	
Ortho-amphibole			x						x	x	x					x	x			x
Epidote		x																		

Type specimen	1	2	3	4	5	6	7	8	9	10	11	12	13	14	15	16	17	18	19	20	21	22	24	27	28
On Fig. 8			25			16	17							23											

Common alteration and accessory minerals include Carbonate, Chlorite, Sericite, Pyrite, Epidote, Tourmaline, Rutile, Zircon, Sphene, Apatite, Iron Oxides and Sulfides. m = minor constituent.

Table II. Plagioclase analyses

	73 1	73 2	GP2 1	GP2 2	GP3 1	GP3 2	GP4 1	GP4 2	G1R 1	G1R 2	S11A 1	S11A 2	W4A 1	W4A 2
SiO ₂	47.43	48.84	51.84	52.03	49.50	49.04	60.13	60.17	56.23	57.31	61.54	61.46	57.46	56.82
Al ₂ O ₃	30.74	31.10	30.87	30.66	31.79	32.02	25.29	24.77	27.77	27.02	25.28	25.01	26.93	27.74
CaO	17.01	16.07	14.25	14.24	15.46	15.91	6.94	7.33	10.45	9.69	7.33	7.23	9.69	9.13
Na ₂ O	1.85	2.39	3.65	3.62	2.79	2.55	7.35	7.52	6.15	6.70	7.78	7.78	6.18	5.23
K ₂ O	0.04	0.05	0.06	0.05	0.03	0.04	0.13	0.14	0.09	0.08	0.14	0.09	0.11	1.06
TOTAL	97.07	98.45	100.67	100.60	99.57	99.56	99.84	99.93	100.69	100.80	102.07	101.57	100.37	99.98
Ions on the basis of 32 (O)														
Si	8.97	9.07	9.37	9.40	9.08	9.01	10.71	10.74	10.06	10.23	10.75	10.78	10.27	10.20
Al	6.85	6.81	6.57	6.53	6.87	6.93	5.31	5.21	5.86	5.68	5.20	5.17	5.68	5.87
Ca	3.45	3.20	2.76	2.76	3.04	3.13	1.32	1.40	2.01	1.85	1.37	1.36	1.86	1.76
Na	0.68	0.86	1.28	1.27	0.99	0.91	2.54	2.60	2.13	2.32	2.63	2.65	2.14	1.82
K	0.01	0.01	0.01	0.01	0.01	0.01	0.03	0.03	0.02	0.02	0.03	0.02	0.03	0.24
Mol. %														
Or	0.3	0.3	0.2	0.3	0.2	0.2	0.7	0.8	0.5	0.5	0.7	0.5	0.7	6.3
Ab	16.4	21.1	31.6	31.4	24.5	22.5	65.3	65.0	51.2	55.4	65.3	65.8	53.1	47.6
An	83.3	78.6	68.2	68.3	75.3	77.3	34.0	34.2	48.3	44.1	34.0	33.7	46.2	46.1
Range	75.7	84.7	66.8	70.3	72.8	83.3	30.0	50.5	38.8	57.3	29.0	56.7	37.3	59.1
Ions on the basis of 32 (O)														
Si	63.42	65.56	57.05	56.64	58.36	59.93	67.42	66.03	61.82	61.60	57.50	57.14	57.14	57.14
Al ₂ O ₃	23.58	23.60	26.33	26.93	25.69	24.68	20.38	21.47	23.20	23.70	25.53	25.82	25.82	25.82
CaO	5.14	5.21	9.10	9.82	8.17	6.97	0.30	0.96	5.29	5.85	8.15	8.23	8.23	8.23
Na ₂ O	9.75	8.92	6.40	5.96	6.87	7.55	11.89	11.03	8.14	8.11	7.08	6.98	6.98	6.98
K ₂ O	0.05	0.04	0.05	0.05	0.05	0.05	0.04	0.06	0.07	0.08	0.07	0.10	0.10	0.10
TOTAL	100.94	101.33	98.93	99.40	99.38	99.38	100.03	99.55	98.52	99.34	98.33	98.27	98.27	98.27
Ions on the basis of 32 (O)														
Si	11.12	11.11	10.34	10.23	10.52	10.73	12.05	11.86	11.10	10.99	10.47	10.41	10.41	10.41
Al	4.87	4.86	5.62	5.73	5.46	5.25	4.33	4.58	4.91	4.99	5.48	5.55	5.55	5.55
Ca	0.96	0.98	1.77	1.90	1.58	1.34	0.06	0.19	1.02	1.12	1.59	1.61	1.61	1.61
Na	2.97	3.02	2.25	2.09	2.40	2.62	4.04	3.77	2.83	2.81	2.50	2.47	2.47	2.47
K	0.01	0.01	0.01	0.01	0.01	0.01	0.01	0.01	0.02	0.02	0.02	0.02	0.02	0.02
Mol. %														
Or	0.2	0.3	0.3	0.2	0.2	0.2	0.2	0.3	0.5	0.5	0.5	0.5	0.5	0.5
Ab	75.4	75.3	55.8	52.3	60.2	66.0	98.3	94.9	73.1	71.1	60.8	60.2	60.2	60.2
An	24.4	24.4	43.9	47.5	39.6	33.8	1.5	4.8	26.4	28.4	38.7	39.3	39.3	39.3
Range	23.5	24.9	43.1	50.6	31.9	43.9	0.3	8.5	20.4	32.1	35.2	44.3	44.3	44.3

Analysts, M. D. Clark and B. Wilson
Range is given in mol. % An.

Key to Analyses in Table

Cordierite-Anthophyllite Rocks and associated Mafic Schists

- BA1C Cordierite-anthophyllite rock (+ quartz, biotite, garnet); Bright Angel Creek.
- 17D-71 Cordierite-anthophyllite rock (+ quartz, biotite, garnet); Travertine Canyon.
- 8H Cordierite-anthophyllite rock (+ quartz, biotite); Travertine Canyon.
- BA2N Anthophyllite-cummingtonite mafic schist; Bright Angel Creek.
- F3B Garnet-cummingtonite rock (+ quartz, biotite); Pipe Creek.

Amphibolite Dykes

- S3 Hornblende-bearing dyke; mile 115.0.
- G1R Hornblende-bearing dyke; mile 115.0
- 57-2F Tremolite-bearing dyke; mile 82.9.

Table III. Calcic amphibole analyses

	O1B 1	O1B 2	S3 1	S3 2	G1R 1	G1R 2	S11A 1	S11A 2	17A-71 1	17A-71 2	17B-71 1	17B-71 2	W4A 1	W4A 2	73 1	73 2	GP2 1	GP2 2	GP3 1	GP3 2	57-2P 1	57-2P 2
SiO ₂	47.53	47.75	43.41	43.71	43.28	43.59	41.74	42.54	42.28	42.17	42.84	42.92	46.43	46.99	52.00	52.17	48.28	47.69	51.77	50.81	52.16	50.87
TiO ₂	0.57	0.55	0.90	0.85	0.89	0.89	0.57	0.80	0.65	0.64	0.66	0.64	0.59	0.62	0.17	0.07	0.60	0.52	0.28	0.33	0.08	0.18
Al ₂ O ₃	7.37	7.40	11.69	11.61	11.33	11.33	15.53	12.32	13.86	13.94	12.97	12.75	11.81	11.56	4.72	4.64	8.39	8.91	4.82	5.60	2.92	4.56
FeO	17.60	17.58	17.36	17.24	18.73	18.48	21.07	21.12	18.86	18.75	17.66	17.88	13.23	13.04	9.42	9.27	13.31	13.60	11.02	11.84	8.05	9.16
MnO	0.41	0.40	0.28	0.28	0.32	0.32	0.55	0.53	0.42	0.42	0.38	0.44	0.31	0.30	0.23	0.20	0.30	0.29	0.26	0.28	0.40	0.39
MgO	10.84	10.97	9.68	9.59	9.12	9.03	6.24	6.74	7.32	7.31	8.43	8.50	12.08	12.19	16.10	15.59	13.39	12.84	15.13	14.87	18.87	18.14
CaO	12.18	12.28	11.53	11.52	11.76	11.90	11.76	11.99	10.98	10.93	11.05	10.98	11.85	11.78	12.87	12.63	12.29	12.33	13.02	12.56	11.00	10.65
Na ₂ O	0.94	0.89	1.19	1.15	1.39	1.38	1.23	1.13	1.40	1.36	1.32	1.36	0.96	0.96	0.55	0.59	0.88	0.88	1.44	0.62	0.73	0.95
K ₂ O	0.45	0.58	0.37	0.34	0.69	0.70	0.96	1.07	0.39	0.39	0.35	0.34	0.31	0.36	0.28	0.25	0.50	0.54	0.25	0.33	0.03	0.08
TOTAL	97.89	98.40	96.41	96.29	97.51	97.42	97.65	98.24	96.16	95.91	95.66	95.81	97.57	97.80	96.34	95.41	97.95	97.60	97.99	97.24	94.24	94.98
Ions on the basis of 23 (O)																						
Si	7.08	7.08	6.58	6.62	6.56	6.57	6.40	6.49	6.46	6.46	6.54	6.55	6.77	6.82	7.51	7.59	7.03	6.98	7.44	7.37	7.63	7.43
Ti	0.06	0.06	0.10	0.10	0.10	0.10	0.07	0.09	0.07	0.07	0.08	0.07	0.06	0.07	0.02	0.01	0.07	0.06	0.03	0.04	0.01	0.02
Al	1.29	1.29	2.09	2.07	2.02	2.02	2.44	2.21	2.50	2.52	2.33	2.29	2.03	1.98	0.80	0.80	1.44	1.54	0.82	0.96	0.50	0.79
Fe	2.19	2.18	2.20	2.18	2.37	2.34	2.70	2.69	2.41	2.40	2.26	2.28	1.61	1.58	1.14	1.13	1.62	1.67	1.32	1.44	0.98	1.12
Mn	0.05	0.05	0.04	0.04	0.04	0.04	0.07	0.07	0.05	0.05	0.05	0.06	0.04	0.04	0.03	0.02	0.04	0.04	0.03	0.03	0.05	0.05
Mg	2.41	2.42	2.19	2.17	2.06	2.04	1.43	1.53	1.67	1.67	1.92	1.94	2.62	2.64	3.47	3.38	2.91	2.80	3.24	3.21	4.11	3.95
Ca	1.94	1.95	1.87	1.87	1.91	1.93	1.93	1.96	1.80	1.79	1.81	1.80	1.85	1.83	1.99	1.97	1.92	1.93	2.01	1.95	1.72	1.67
Na	0.27	0.26	0.35	0.34	0.41	0.41	0.36	0.34	0.41	0.40	0.39	0.40	0.27	0.27	0.15	0.17	0.25	0.25	0.40	0.17	0.21	0.27
K	0.09	0.11	0.07	0.07	0.13	0.13	0.19	0.21	0.08	0.08	0.07	0.07	0.06	0.07	0.05	0.05	0.09	0.10	0.05	0.06	0.01	0.02
Mg	0.518	0.520	0.494	0.494	0.461	0.462	0.341	0.357	0.404	0.405	0.454	0.453	0.614	0.620	0.748	0.746	0.637	0.621	0.706	0.686	0.800	0.772
Mg+Fe+Mn Al+Na+K	0.413	0.415	0.628	0.620	0.640	0.640	0.748	0.690	0.748	0.750	0.698	0.690	0.590	0.580	0.250	0.255	0.445	0.473	0.318	0.298	0.180	0.270

Analysts, M. D. Clark and R. Wilson

Table IV. Anthophyllite, Gedrite and Cummingtonite analyses

	BA2N 1	BA2N 2	SH 1	SH 2	17D-71 1	17D-71 2	17D-71 3	BA1C 1	BA1C 2	BA2N 1	BA2N 2	BA2N 3	FSB 1	FSB 2	17A-71 1	17A-71 2	17B-71 1	17B-71 2
SiO ₂	51.84	51.76	52.45	52.47	52.39	45.99	42.88	43.12	42.99	54.82	54.53	54.82	53.22	53.46	52.99	52.97	53.12	52.91
TiO ₂	0.17	0.19	0.06	0.09	0.04	0.14	0.14	0.16	0.13	0.05	0.06	0.05	0.04	0.03	0.01	0.05	0.02	0.00
Al ₂ O ₃	5.06	5.08	2.49	3.01	3.04	11.37	15.99	15.40	16.17	1.39	1.55	1.27	1.06	0.75	0.80	0.84	0.77	0.66
FeO	23.12	23.23	22.70	22.67	24.86	24.68	24.34	23.40	22.97	23.33	23.18	23.17	25.78	25.12	26.39	26.33	25.07	25.89
MnO	0.62	0.61	0.49	0.54	0.22	0.19	0.21	0.14	0.14	0.59	0.62	0.58	0.05	0.05	1.14	1.16	1.27	1.21
MgO	16.57	16.71	17.40	17.44	16.61	13.07	11.48	12.63	12.39	17.76	17.61	17.63	16.46	16.91	14.47	14.32	15.10	15.08
CaO	0.26	0.27	0.18	0.21	0.21	0.30	0.41	0.23	0.17	0.27	0.30	0.30	0.05	0.05	0.77	0.76	0.68	0.71
Na ₂ O	0.60	0.67	0.18	0.23	0.30	1.10	1.72	1.74	1.85	0.10	0.09	0.08	0.05	0.05	0.06	0.13	0.10	0.05
K ₂ O	0.00	0.01	0.00	0.00	0.01	0.00	0.01	0.02	0.01	0.00	0.00	0.00	0.01	0.00	0.01	0.01	0.02	0.02
TOTAL	98.24	98.53	95.95	96.66	97.68	96.84	96.78	96.84	96.82	98.31	97.94	97.90	96.72	96.42	96.64	96.57	96.15	96.53
Ions on the basis of 23 (O)																		
Si	7.53	7.51	7.78	7.72	7.70	6.87	6.43	6.43	6.40	7.93	7.92	7.95	7.92	7.95	7.97	7.97	7.98	7.96
Ti	0.02	0.02	0.01	0.01	0.00	0.02	0.02	0.02	0.01	0.01	0.01	0.01	0.00	0.00	0.00	0.00	0.00	0.00
Al	0.87	0.87	0.44	0.52	0.53	2.00	2.76	2.71	2.84	0.24	0.26	0.22	0.19	0.13	0.14	0.15	0.14	0.12
Fe	2.81	2.82	2.81	2.79	3.06	3.08	3.05	2.92	2.86	3.82	3.81	3.81	3.21	3.12	3.32	3.31	3.15	3.26
Mn	0.08	0.07	0.06	0.07	0.03	0.02	0.02	0.02	0.02	0.07	0.08	0.07	0.01	0.01	0.15	0.15	0.16	0.15
Mg	3.59	3.61	3.85	3.83	3.64	2.91	2.57	2.81	2.75	3.83	3.81	3.81	3.65	3.75	3.24	3.21	3.38	3.38
Ca	0.04	0.04	0.03	0.03	0.03	0.05	0.07	0.04	0.03	0.04	0.05	0.05	0.01	0.01	0.12	0.12	0.11	0.11
Na	0.17	0.19	0.05	0.07	0.08	0.32	0.50	0.50	0.53	0.03	0.02	0.02	0.01	0.02	0.02	0.04	0.03	0.01
K	0.00	0.00	0.00	0.00	0.00	0.00	0.00	0.00	0.00	0.00	0.00	0.00	0.00	0.00	0.00	0.00	0.00	0.00

Analysts, M. D. Clark and R. Wilson

Early Amphibolites.

- S11A Hornblende mafic schist; Clear Creek.
- W4A Hornblende mafic schist; Waltherberg Canyon.
- 17A-71 Hornblende mafic schist (+ cummingtonite, garnet); Travertine Canyon.
- 17B-71 Hornblende mafic schist (+ cummingtonite); Travertine Canyon.

Other Rocks.

- B11A Garnet-biotite schist; Boucher Creek.
- B12B Garnet-biotite-chlorite schist; Boucher Creek.
- O1B Tonalite, Diamond Creek pluton; mile 22.9.

Granite Park Mafic Complex (mile 20q)

- 73 Meta-troctolite-gabbro.
- GP2 Amphibolite.
- GP3 Anorthosite.
- GP4 Trondhjemite.

Table VI. Cordierite, Biotite and Talc analyses

	BA1C 1	BA1C 2	8H 1	8H 2	17A-71 1	O1B 1	O1B 2	S11A 1	S11A 2	W4A 1	W4A 2	17A-71 1	P5B 1	P5B 2	8H 1	BA1C 1	BA1C 2	57-2P 1	57-2P 2
SiO ₂	49.04	48.81	48.93	48.93	48.69	36.96	37.35	36.54	36.56	37.96	38.02	35.82	37.16	36.93	37.41	37.75	37.84	59.29	59.50
TiO ₂	0.01	0.02	0.00	0.01	0.00	1.44	1.50	2.39	2.47	1.68	1.63	2.70	1.57	1.51	1.58	1.25	1.38	0.10	0.04
Al ₂ O ₃	32.41	32.43	33.03	33.01	31.98	16.46	17.59	16.41	16.45	16.55	16.79	16.60	17.67	17.61	18.29	17.71	17.67	0.75	0.78
FeO	5.60	5.61	6.04	5.94	6.76	20.75	19.34	21.88	22.30	14.60	14.70	19.34	18.10	17.94	15.07	14.63	14.81	5.59	5.70
MnO	0.05	0.06	0.16	0.13	0.07	0.31	0.26	0.33	0.36	0.11	0.11	0.11	0.01	0.02	0.06	0.01	0.02	0.06	0.06
MgO	9.65	9.62	9.74	9.65	9.12	10.62	10.58	8.93	8.71	14.53	14.41	10.32	12.33	12.52	13.51	14.54	14.56	28.08	28.03
CaO	0.01	0.03	0.01	0.01	0.01	0.06	0.02	0.00	0.01	0.01	0.00	0.06	0.01	0.00	0.02	0.00	0.00	0.01	0.00
Na ₂ O	0.31	0.30	0.17	0.17	0.18	0.09	0.11	0.11	0.09	0.06	0.05	0.24	0.43	0.41	0.43	0.45	0.49	0.14	0.04
K ₂ O	0.01	0.02	0.01	0.01	0.01	8.70	9.17	9.01	9.06	8.99	9.18	8.29	8.01	8.14	8.39	8.06	8.03	0.06	0.01
TOTAL	97.09	96.90	98.09	97.86	96.82	95.39	95.92	95.60	96.01	94.49	94.89	93.48	95.29	95.08	94.76	94.40	94.80	94.08	93.66
Ions on the basis of 18 (O) or 24 (O, OH, F)																			
Si	5.05	5.04	5.00	5.01	5.05	6.15	6.13	6.11	6.10	6.18	6.17	6.04	6.07	6.05	6.09	6.11	6.11	8.70	8.83
Ti	0.00	0.00	0.00	0.00	0.00	0.18	0.18	0.30	0.31	0.21	0.20	0.34	0.19	0.19	0.19	0.15	0.17	0.01	0.00
Al	3.93	3.95	3.98	3.98	3.91	3.23	3.40	3.24	3.24	3.17	3.21	3.30	3.40	3.40	3.51	3.38	3.36	0.13	0.05
Fe	0.48	0.48	0.52	0.51	0.59	2.89	2.65	3.06	3.11	1.99	1.99	2.73	2.47	2.46	2.05	1.98	2.00	0.69	0.71
Mn	0.00	0.00	0.01	0.01	0.01	0.04	0.04	0.05	0.05	0.01	0.01	0.02	0.00	0.00	0.01	0.00	0.00	0.01	0.01
Mg	1.48	1.48	1.48	1.47	1.41	2.63	2.59	2.23	2.17	3.52	3.49	2.60	3.00	3.06	3.28	3.51	3.50	6.06	6.06
Ca	0.00	0.00	0.00	0.00	0.00	0.01	0.00	0.00	0.00	0.00	0.00	0.01	0.00	0.00	0.00	0.00	0.00	0.00	0.00
Na	0.06	0.06	0.03	0.03	0.04	0.03	0.03	0.03	0.03	0.02	0.02	0.08	0.14	0.13	0.14	0.14	0.15	0.04	0.01
K	0.00	0.00	0.00	0.00	0.00	1.84	1.92	1.92	1.93	1.87	1.90	1.78	1.67	1.70	1.79	1.66	1.65	0.01	0.00

Analysts, M. D. Clark and R. Wilson

Table V. Garnet analyses

	BA1C 1R	BA1C 1C	BA1C 1M	BA1C 2R	BA1C 2C	BA1C 2M	P5B 1M	17A-71 1R	17A-71 1C	17A-71 1M	17A-71 2R	17A-71 2C	17A-71 2M	B12B 1R	B12B 1C	B12B 1M
SiO ₂	38.14	38.66	38.37	38.41	38.61	38.55	38.33	38.55	38.60	38.44	38.35	38.48	38.42	36.90	37.16	36.98
TiO ₂	0.00	0.00	0.01	0.00	0.00	0.01	0.01	0.00	0.04	0.02	0.00	0.06	0.03	0.00	0.15	0.07
Al ₂ O ₃	21.51	21.63	21.64	21.50	21.49	21.61	21.50	21.34	21.47	21.36	21.32	21.18	21.28	20.93	21.09	21.09
FeO	35.71	33.34	34.26	34.56	32.99	33.47	36.72	28.62	26.98	28.09	28.72	26.97	27.90	33.43	25.63	29.80
MnO	0.73	0.57	0.63	0.68	0.59	0.63	0.28	5.68	5.70	5.54	5.42	5.63	5.60	2.07	5.23	3.41
MgO	4.07	6.01	5.23	5.03	6.26	5.87	4.06	2.05	2.15	2.21	2.24	2.13	2.17	1.75	1.55	1.62
CaO	1.12	1.04	1.06	0.96	0.88	0.97	0.47	4.68	6.79	5.50	4.66	6.33	5.46	3.36	8.34	5.90
TOTAL	101.28	101.25	101.20	101.15	100.82	101.11	101.37	100.92	101.73	101.16	100.71	100.78	100.86	98.44	99.13	98.86
Ions on the basis of 24 (O)																
Si	6.02	6.03	6.01	6.03	6.03	6.02	6.04	6.10	6.05	6.07	6.08	6.08	6.08	6.04	5.99	6.00
Ti	0.00	0.00	0.00	0.00	0.00	0.00	0.00	0.00	0.00	0.00	0.00	0.01	0.00	0.00	0.02	0.01
Al	4.00	3.97	4.00	3.98	3.96	3.98	4.00	3.98	3.97	3.97	3.99	3.95	3.97	4.03	4.01	4.03
Fe	4.71	4.35	4.49	4.54	4.31	4.37	4.84	3.79	3.54	3.71	3.81	3.57	3.69	4.57	3.45	4.05
Mn	0.10	0.07	0.08	0.09	0.08	0.08	0.04	0.76	0.76	0.74	0.73	0.75	0.75	0.29	0.71	0.47
Mg	0.96	1.40	1.22	1.18	1.46	1.37	0.96	0.48	0.50	0.52	0.53	0.50	0.51	0.43	0.37	0.39
Ca	0.19	0.17	0.18	0.16	0.15	0.16	0.08	0.79	1.14	0.93	0.79	1.07	0.93	0.59	1.44	1.03
Almandine	79.12	72.41	75.17	76.06	71.65	73.01	81.89	65.01	59.58	62.87	65.02	60.49	62.78	77.84	57.77	68.19
Pyrope	16.06	23.43	20.46	19.72	24.57	22.88	16.15	8.31	8.46	8.80	9.02	8.53	8.70	7.27	6.22	6.59
Grossularite	3.17	2.91	2.97	2.72	2.48	2.73	1.33	13.62	19.21	15.76	13.55	18.20	15.75	10.01	24.08	17.30
Spessartine	1.65	1.25	1.41	1.50	1.32	1.39	0.62	13.06	12.75	12.56	12.43	12.79	12.77	4.98	11.93	7.91
% assigned	99.42	99.39	99.05	99.58	99.04	99.57	98.82	97.68	99.20	98.67	98.09	98.68	98.45	98.25	99.71	99.02